

26

THE SPATIAL DISTRIBUTION OF INFRARED RADIATION FROM VISIBLE REFLECTION NEBULAE

L. Luan¹, M.W. Werner², E. Dwek³, and K. Sellgren⁴

¹Astronomy Department, University of California at Berkeley

²NASA-Ames Research Center

³NASA-Goddard Space Flight Center

⁴Institute for Astronomy, University of Hawaii

I. Introduction

The emission at IRAS $12\mu\text{m}$ and $25\mu\text{m}$ bands of reflection nebulae is far in excess of that expected from the longer wavelength equilibrium thermal emission (Sellgren *et al.* 1987). The excess emission in the IRAS $12\mu\text{m}$ band is a general phenomenon, seen in various components of interstellar medium such as infrared cirrus clouds (Boulanger *et al.* 1985; Weiland *et al.* 1986), reflection nebulae (Castelaz *et al.* 1987; Sellgren *et al.* 1987), HII regions, atomic and molecular clouds (Boulanger and Pérault 1988), and also normal spiral galaxies (Helou 1986). This excess emission has been attributed to ultraviolet-excited fluorescence in polycyclic aromatic hydrocarbon (PAH) molecules (Léger and Puget 1984; Allamandola *et al.* 1985) or to the effect of temperature fluctuations in very small grains (Draine and Anderson 1985; Weiland *et al.* 1986).

We present here results to date of studies of IRAS data on reflection nebulae selected from the van den Bergh (1966) reflection nebula sample and the van den Bergh and Herbst (1975) reflection nebula sample. Detailed scans of flux ratio and color temperature across the nebulae were obtained in order to study the spatial distribution of infrared emission. We have used a model to predict the spatial distribution of infrared emission from dust grains illuminated by a B-type star. We have also used the model to explore the excitation of the IRAS $12\mu\text{m}$ band emission as a function of stellar temperature. Our model predictions are in good agreement with the analysis of reflection nebulae, illuminated by stars with stellar temperature ranging from 21,000K down to 3,000K, presented at this meeting by Sellgren.

II. Data Processing and Results

We have used co-added intensity images at $12\mu\text{m}$, $25\mu\text{m}$, $60\mu\text{m}$ and $100\mu\text{m}$ obtained from the IRAS data-base. All data have been smoothed to the IRAS $100\mu\text{m}$ band resolution ($3' \times 5'$) using an algorithm developed by W. Rice at IPAC; this facilitates comparison between different IRAS channels.

For each nebula, we obtained a $2.5^\circ \times 2.5^\circ$ field with the nebula located at the center. The sizes of the nebulae in our study vary from 15 to 45 arcminutes. The large field makes it easier to subtract the global background emission. Zodiacal light and galactic emission were removed by fitting a plane to all bands, based on the fact that the zodiacal light and galactic emission are large scale features. Local background was measured using four $3' \times 3'$ boxes around the nebula. The standard deviation in the background measurements defined a $3\text{-}\sigma$ threshold to exclude the outermost regions of the nebula, where the excitation contribution from

other sources, e.g. interstellar radiation field and sometimes nearby stars, may be comparable to that of the illuminating starlight. The flux ratios thus obtained reveal the spatial distribution of nebular colors as a function of the intensity of the radiation field of the illuminating star.

Flux ratios obtained for three reflection nebulae are shown in Figure 1a, 1b and 1c, for NGC7023 (illuminating star spectral type B5, apparent visual magnitude $m_V=7.39$); Merope Nebula (B6, $m_V=4.18$) and vdB10 (A0, $m_V=5.81$), respectively. They all show that $F_\nu(60)/F_\nu(100)$ decreases as distance from the star increases. This is expected from emission from large grains which are heated in thermal equilibrium by starlight. On the other hand, the high values of $F_\nu(12)/F_\nu(25)$ even in the outer regions of the nebulae are far in excess of what is expected from equilibrium thermal emission.

The scan line across the Merope Nebula we used was close to that adopted by Castelaz *et al.* (1987), and almost the same answers were obtained. In vdB10, the stellar type of the illuminating star is A0, but $F_\nu(60)/F_\nu(100)$ shows higher values, which imply higher temperature of grains, compared with the Merope nebula which is illuminated by a B star. This may be due to the fact that vdB10 is much less spatially extended than NGC7023 and the Merope Nebula, where dust grains at different distances along the line of sight contribute to the flux. In vdB10, this effect is much smaller, so the flux observed represents more closely the nebular emission from the immediate vicinity of the star. In some cases of our reflection nebulae sample, $F_\nu(12)/F_\nu(25)$ ratio goes down significantly at the position of the star, as seen in vdB10 (Figure 1c). Examples of this phenomenon occur more frequently in reflection nebulae illuminated by OB stars and with smaller angular sizes, where the emission from dust grains in high energy density radiation field is less diluted by the layers of dust grains along the line of sight. The decrease in the $F_\nu(12)/F_\nu(25)$ ratio in regions of high starlight energy density may be attributable to the destruction of $12\mu\text{m}$ band emitters (Ryter *et al.* 1987; Boulanger *et al.* 1988), and/or to the enhancement of $25\mu\text{m}$ band equilibrium-emission from large grains as they are hotter in the vicinity of the star.

Simple models in which all geometrical effects are ignored predict that the $60\mu\text{m}/100\mu\text{m}$ temperature should vary with θ , as $\log T_c(60/100) \sim -k \log \theta$ ($k=2/(4+n)$). Here θ is the angular offset from the star and n is the exponent of the grain emissivity power law ($Q(\lambda) \sim 1/\lambda^n$). For n between 1 and 2, the commonly adopted range, we expect that the temperature to vary inversely as the .33 to .40 power of the angle. In Figure 3, we show $T_c(60/100)$ vs θ for four nebulae. The data are well fit by straight lines with slopes between .25 and .41, consistent with the theoretical expectation. This provides further evidence for equilibrium thermal emission as the explanation of the 60-to-100 μm radiation.

III. Model Calculations

The model we used incorporates the conventional MRN (Mathis, Rumpl, and Nordsieck 1977) size distribution which is a graphite and silicate grain mixture with a power law size distribution $n(a)=n_0 a^{-3.5}$ as the large grain component, with size range extended to cover $50\text{\AA} < a \leq 1\mu\text{m}$, together with an enhanced population of

graphite grains with $n(a)=n_0 a^{-5.0}$ and $3\text{\AA} \leq a \leq 50\text{\AA}$, as the small grain component. In the studies of high galactic latitude infrared cirrus clouds (Weiland *et al.* 1986) and reflection nebulae in the Pleiades (Werner *et al.* 1988), this enhanced small grain population was needed to fit the IRAS data. Small silicate grains are not included in the small grain component because the silicate $9.6\mu\text{m}$ emission feature is not observed in reflection nebulae (Sellgren *et al.* 1985). The mass ratio of small grains ($a \leq 50\text{\AA}$), to large grains ($a > 50\text{\AA}$), are assume to be 0.5 in all cases. The model predictions of flux ratio $F_\nu(12)/F_\nu(25)$ and $F_\nu(60)/F_\nu(100)$ for dust illuminated by a B1.5 star and visual magnitude $m_V = 7$ are shown in Figure 2. The effect of temperature fluctuations in the very small grain dominates the $F_\nu(12)/F_\nu(25)$ ratio. $F_\nu(60)/F_\nu(100)$ is dominated by the equilibrium emission from the large grains. Also in this model, we predict appreciable values for the ratio $R = \nu F_\nu(12)/\nu F_\nu(100)$ even for stars with effective temperature below 5000K. Figure 4 is the result of calculation of stellar spectral types ranging from B0 to M5, with fixed angular offset $\theta = 3'$ and visual magnitude $m_V = 8$. Thus in this model, the fraction of the stellar energy radiated in the ultraviolet (below 2500\AA , for example), falls much more rapidly with spectral type than does the fraction of the absorbed stellar radiation reradiated at $12\mu\text{m}$ band.

IV. Conclusions

1. The $100\mu\text{m}$ and $60\mu\text{m}$ band emission of reflection nebulae show the behavior expected from thermal emission from large dust grains which are in thermal equilibrium, heated by the illuminating stars of the nebulae. On the other hand, for the cooler diffuse interstellar medium, which is heated by the diffuse interstellar radiation field, there is considerable amount of non-equilibrium emission in $60\mu\text{m}$ band from small grain components (Draine and Anderson 1985).
2. The $12\mu\text{m}$ and a large part of the $25\mu\text{m}$ band emission are produced in a non-equilibrium process. The independence of the ratio $F_\nu(12)/F_\nu(25)$ of the intensity of the starlight is expected from temperature fluctuations in very small grains. In some cases, $F_\nu(12)/F_\nu(25)$ decreases significantly in the immediate vicinity of the illuminating star. Careful comparison between analysis of IRAS data and model calculation may help to distinguish if the decrease of $F_\nu(12)/F_\nu(25)$ in the immediate vicinity of the illuminating star is attributable to dust destruction or merely to enhancement of thermal emission at of $25\mu\text{m}$.
3. A two-component model of dust grains, including the effect of temperature fluctuations of very small grains, predicts that the excess $12\mu\text{m}$ emission is readily excited by photons softer than the ultraviolet, in agreement with the data presented at this meeting by Sellgren. This agreement suggest that a broad range of photon energies intending into the visual is capable of exciting the excess $12\mu\text{m}$ emission.

Acknowledgements

We thank Dr. Allamondola for helpful discussions. LL specially thank Professor Heiles for many helpful discussions. This work was supported by IPAC and by NASA-Ames Consortium Agreement NCA2-269.

References

- Allamandola, L.J., Tielens, A.G.G.M., and Barker, J.R. 1985, *Ap.J.Lett.*, **315**, L61.
- van den Bergh, S. 1966, *Astron.J.*, **71**, 990.
- van den Bergh, S., and Herbst, W. 1975, *Astron.J.*, **80**, 208.
- Boulanger, F., Baud, B., and van Albada, G.D. 1985, *Astr.Ap.Lett.*, **144**, L93.
- Boulanger, F., and Pérault, M. 1988, *Ap.J.*, **330**, 964.
- Boulanger, F. *et al.* 1988, *Ap.J.*, to be published.
- Castelaz, M.W., Sellgren, K. and Werner, M.W. 1987, *Ap.J.*, **313**, 853.
- Draine, B.T., and Anderson, N. 1985, *Ap.J.*, **292**, 494.
- Léger, A., and Puget, J.L. 1984, *Astr.Ap.*, **137**, L5.
- Ryter, C., Puget, J.L., and Pérault, M. 1987, *Astr.Ap.*, **186**, 312.
- Sellgren, K., Allamandola, L.J., Bregman, J.D., Werner, M.W., and Wooden, D.H. 1985, *Ap.J.*, **299**, 416.
- Sellgren, K., Castelaz, M.W., Werner, M.W., and Luan, L. 1987, *Proceedings of Third IRAS Conference*, Queen Mary College: to be published.
- Weiland, J.L., Blitz, L., Dwek, E., Hauser, M., Magani, L., Rickard, L.J. 1986, *Ap.J.Lett.*, **306**, L101.

FIGURE CAPTIONS

Figure 1a, 1b, 1c. One-dimensional scans of $F_\nu(12)/F_\nu(25)$ and $F_\nu(60)/F_\nu(100)$ through the central stars for three reflection nebulae NGC7023, Merope Nebula and vdB10, respectively.

Figure 2. Two-component model predictions of $F_\nu(12)/F_\nu(25)$ and $F_\nu(60)/F_\nu(100)$ ratios of dust emission, illuminated by a B1.5 star with apparent visual magnitude $m_V = 7$, as a function of angular offset. The relative roles that two grain components play are clearly shown in $F_\nu(12)/F_\nu(25)$ and $F_\nu(60)/F_\nu(100)$ ratios.

Figure 3. One-dimensional color temperature $T_c(60/100)$ scans (derived from the $60\mu\text{m}$ to $100\mu\text{m}$ flux ratio) through the central stars for four reflection nebulae. The lines, labelled by the slope k ($T_c(60/100)$ varies as angular offset to the $-k$ power), are least-square fits to the data.

Figure 4. Model prediction of IRAS $\nu F_\nu(12)/\nu F_\nu(100)$ ratio of dust emission at a fixed angular offset from star ($\theta = 3'$), as a function of stellar temperature, assuming mass ratio of very small grains to big grains $b=0.5$ and visual magnitude $m_V = 8$. Also plotted are fractions of stellar energy in the ultraviolet (below 2500\AA) and observational data of reflection nebulae presented at this meeting by Sellgren (the arrows represent the upper limits of the data). This result suggest that a broad range of photon energies extending into the visual are capable of exciting the excess $12\mu\text{m}$ emission.

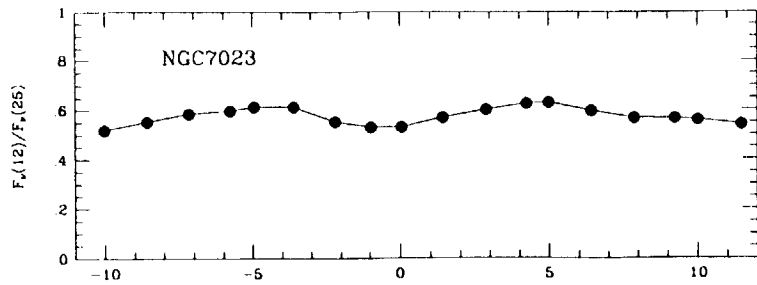


Figure 1a

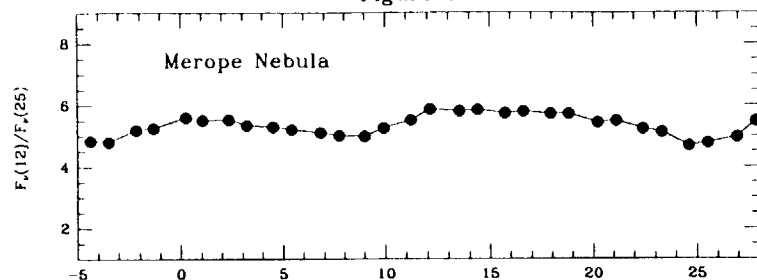


Figure 1b

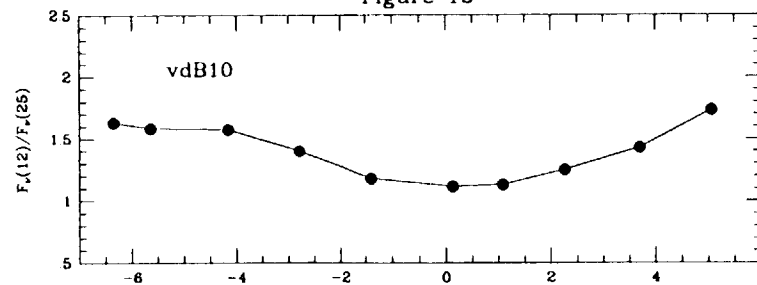


Figure 1c

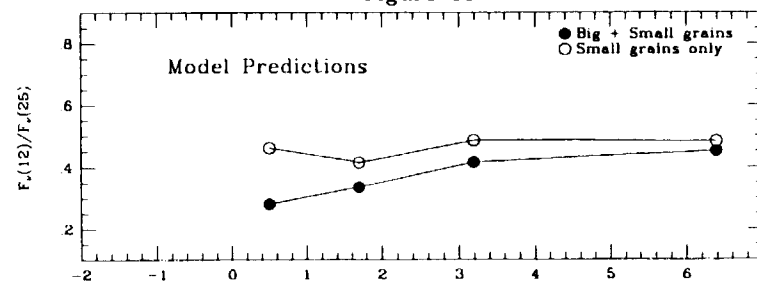


Figure 2

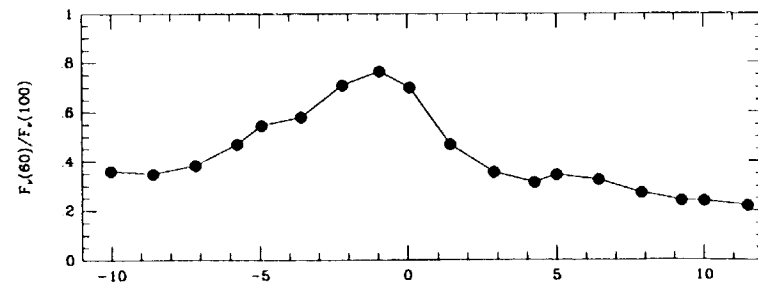


Figure 1a

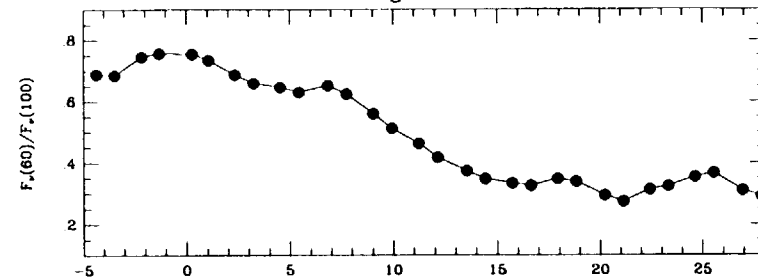


Figure 1b

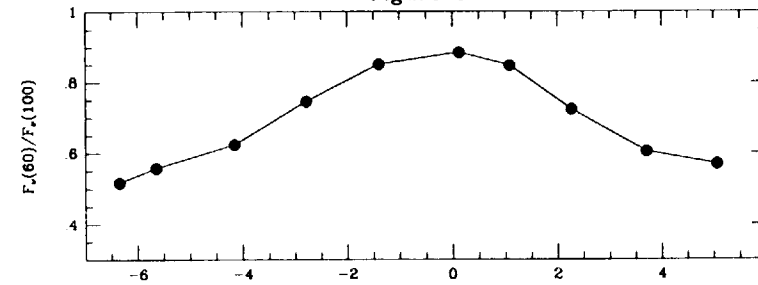


Figure 1c

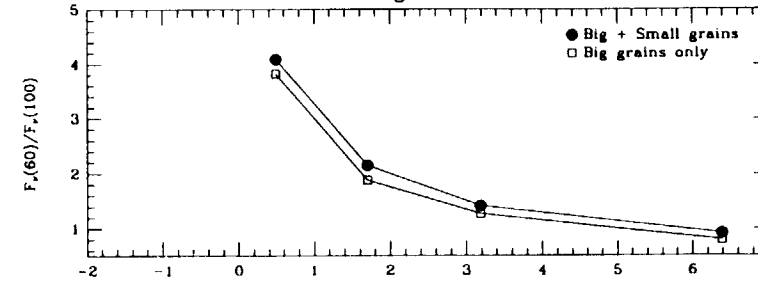


Figure 2

Angular Offset from star (arcmin)

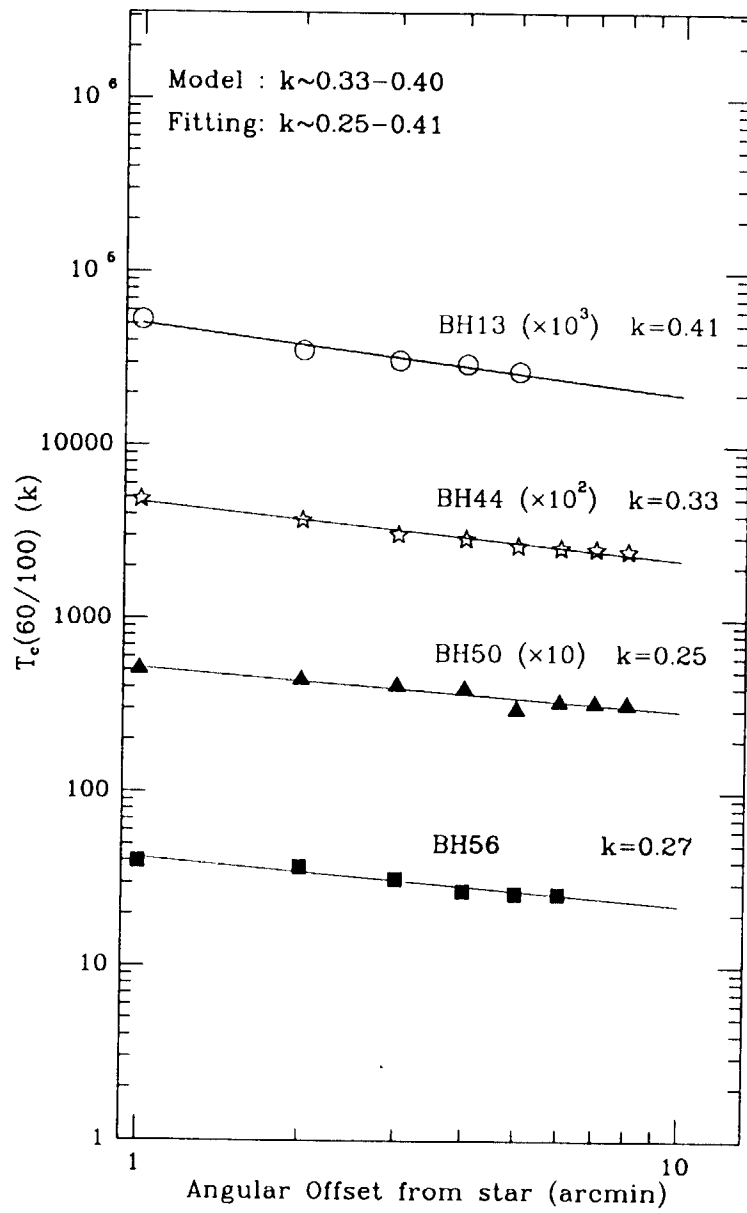


Figure 3

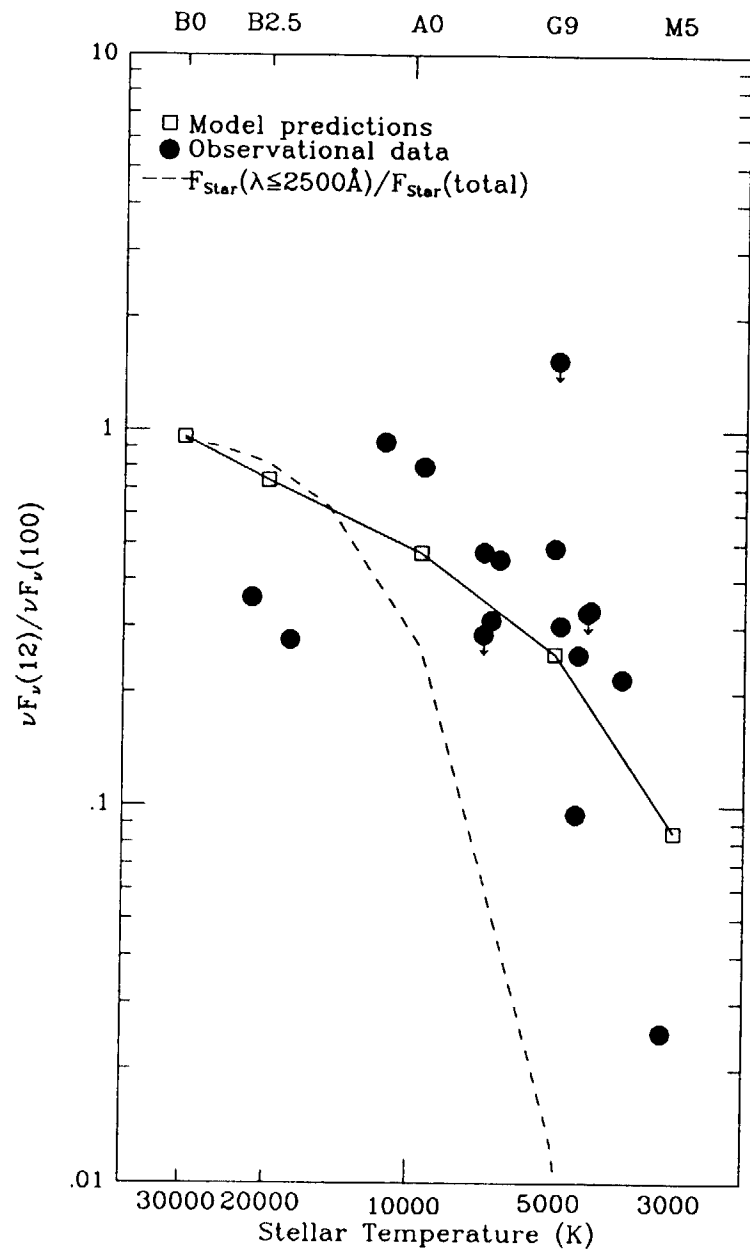


Figure 4